



Multi-port broadband adaptive RF power splitter employing an Opto-VLSI Processor

Haithem A B Mustafa¹, Feng Xiao¹, Kamal Alameh¹ and Feijun Song²

¹Electron Science Research Institute, Edith Cowan University, Australia

²China Daheng Optics Division, China Daheng Group, Beijing, China

A novel multi-port broadband adaptive RF (Radio Frequency) power splitter structure is proposed and experimentally demonstrated. The multi-port broadband RF adaptive power splitter structure employs an Opto-VLSI processor for optical beam multicasting in conjunction with an optical fiber array, a photo-detector array, and an array of 4-f imaging lens system for splitting a broadband RF signal into multiple output RF ports with user-defined splitting ratios. A proof of concept 1×8 broadband adaptive RF power splitter structure, driven by optimized multicasting phase holograms uploaded onto the Opto-VLSI processor, is developed, demonstrating the ability to arbitrarily split an RF signal to various output port with variable power splitting ratios over a wide frequency range. © Anita Publications. All rights reserved.

Keywords: Opto-VLSI processing, R F splitting, Microwave photonics

1 Introduction

RF power splitters are key elements for RF applications requiring adaptive RF signal processing, such as wireless communication systems, beam forming networks and smart antenna systems [1-5]. A multi-port reconfigurable broadband power splitter with variable splitting ratios allows such systems to operate with a high degree of flexibility, thus achieving multiple functions that are not possible with conventional fixed-ratio RF power splitters [6]. Conventional RF power splitters are mainly designed to operate within specific frequency ranges [7]. Various processes, based on CMOS, BiCMOS, MESFET, and printed circuit board (PCB), have been used to develop RF power splitters [8-11]. Typical specifications of a power splitter include the output port count, loss, cost, bandwidth, and size [6]. Broadband RF power splitters based on CMOS technology have recently been reported [12, 13], however, these RF splitters have limited flexibility in terms of achieving arbitrary splitting ratios, while maintaining their broadband operation. A promising approach to splitting a broadband RF signal adaptively into different output ports using Opto-VLSI processing in conjunction with a fiber array and single-lens 4-f imaging system has been reported [14]. The output-port count for the adaptive RF power splitter structure was limited to few ports due to the high insertion loss experienced by the split optical beams routed to the outer fiber ports, where the ability of the Opto-VLSI processor to realizing large beam steering angles is crucial for optimum beam coupling.

In this paper, a novel multi-port broadband adaptive RF power splitter based on Opto-VLSI processing in conjunction with a photodetector array and an array of a 4-f imaging systems (rather than a single lens) is proposed and experimentally demonstrated. Experimental results show that by driving the Opto-VLSI processor with optimized multicasting holograms, a broadband RF signal can be split into many RF output ports with arbitrary power splitting ratios.

2 OPTO-VLSI processor and optical beam multicasting

An Opto-VLSI processor is an electronically-driven adaptive optical diffractive element capable of steering/shaping an incident optical beam without mechanically moving parts. As shown in Figure 1, an Opto-VLSI processor comprises an array of liquid crystal (LC) cells driven by a Very-Large-Scale-Integrated (VLSI) circuit [14-16], which generates discrete voltages across each cell thus inducing digital holographic diffraction gratings that achieve arbitrary optical beam steering or multicasting. A transparent Indium-Tin Oxide (ITO) layer is typically used as the ground electrode, and a quarter-wave-plate (QWP) layer is deposited

Corresponding author :

e-mail: k.alameh@ecu.edu.au (Kamal Alameh)

between the LC and the aluminum mirror (also acts as an electrode) to accomplish polarization-insensitive operation.

A multicasting phase hologram can split an incident optical beam into N output beams with variable intensities along different directions. By using an optimized multicasting phase hologram, a collimated Gaussian beam incident onto the Opto-VLSI processor can adaptively be diffracted along different directions with arbitrary optical power splitting ratios. The beam multicasting resolution, or minimum splitting angle relative to the 0th order diffraction beam, is given by [15]

$$\alpha = \arcsin \frac{\lambda}{N \times d} \quad (1)$$

where λ is the optical wavelength, N is the number of pixels illuminated by the incident optical beam, and d is the pixel pitch.

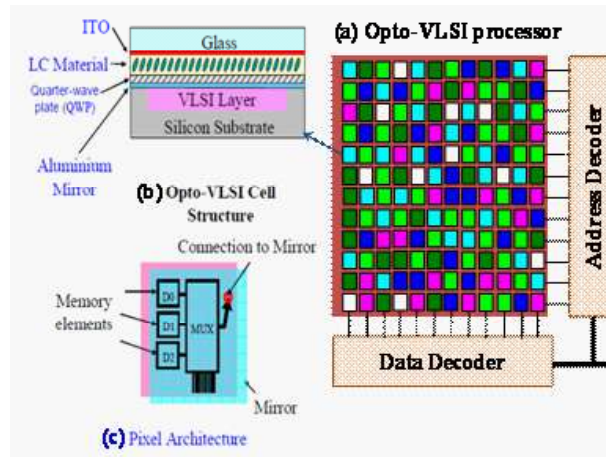


Fig 1.(a) Opto-VLSI processor layout, (b) Opto-VLSI cell structure and (c) pixel architecture.

Several computer algorithms, such as the genetic, simulated annealing, phase encoding, and projection algorithms [17-21], have been used for generating optimized multicasting phase holograms that produce a target far-field distribution, defined by the split beam positions and power levels. For a target splitting ratio profile, an optimised phase hologram can always be generated, which minimizes the 0th order diffracted beam and maximizes the signal-to-crosstalk ratio at every output port.

3 Experimental setup

Figure 2 shows the experimental setup that was used to demonstrate the proof-of-concept of the proposed RF power splitter. The proposed structure consists of an Opto-VLSI processor, a 2-element lens array with adjustable lens spacing, and an optical fiber array. All components were aligned to form two 4-f imaging systems. The Opto-VLSI processor used in the experiments has $1 \times 4,096$ pixels, a pixel size of $(1.0 \mu\text{m} \times 6.0 \text{mm})$, a pixel pitch of $1.8 \mu\text{m}$ (i.e. $0.8 \mu\text{m}$ of dead space between pixels), and an active area of $(7.4 \text{mm} \times 6.0 \text{mm})$. The lens array had two elements of focal length (f) 9mm and diameter 3mm , and was placed between and at an equal distance, f , from both the fiber array and the Opto-VLSI processor. The intensity of a 1550nm continuous wave (CW) laser signal was externally modulated by an RF signal using a JDS Uniphase electro-optic modulator (EOM). The RF-modulated optical signal was amplified by an erbium-doped fiber amplifier (EDFA) and launched, as an input signal, into Port 9 of an optical fiber array of $127 \mu\text{m}$ fiber-to-fiber spacing.

By driving the Opto-VLSI with an optimized multicasting phase hologram, the RF-modulated optical power was split into five output ports, Port 1, Port 2, Port 3, Port 4, and Port 10 (in addition to the 0th

order beam) which propagated along the optimized directions so that they were coupled back into the fiber array output ports through the 4-f imaging system. The output signal of Port 10 was amplified via an EDFA and then launched as a second input into Port 11 to be split into Four output ports: 'Port 5, Port 6, Port 7, and Port 8'. For both input RF-modulated optical beams (at Ports 9 and 11), the split RF-modulated optical beams propagated along $\pm 0.81^\circ$, $\pm 1.62^\circ$, and $\pm 2.43^\circ$ with respect to the direction of the 0th order beam. After emerging from the optical fibers, both input RF-modulated optical signals were collimated through the corresponding lenses, at a diameter of 1.962 mm. Each collimated beam illuminated around independently-addressed 1090 pixels of the Opto-VLSI processor, leading to high diffraction efficiency and high optical splitting angle resolution [15]. The active window of the Opto-VLSI processor was divided into two pixel blocks, separated by 934 un-addressed pixels. A photo detector (PD) array was used to detect the split optical signals emerging from Ports 1-8, and an oscilloscope and a network analyzer were used to measure the corresponding RF output signals and frequency responses, respectively. The RF splitting ratio is typically given by [14]

$$\eta_n = A\alpha_n^2 \quad (2)$$

where α_n is the optical splitting ratios, $n = 1-8$ RF output port, and A is a constant defined by the EOM switching voltage, the optical input power launched into the EOM, the responsivity of the photo detector, the impedance of transimpedance amplifier used after each photo detector, and the EDFA gain [14].

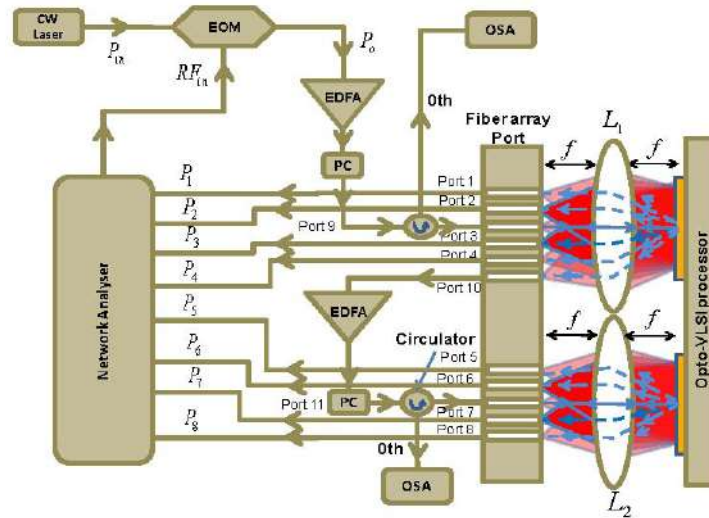


Fig 2. Experimental setup illustrating the proposed broadband adaptive RF splitter structure, which is based on the use of an Opto-VLSI processor in conjunction with an array of 4-f imaging systems.

4 Experimental results and discussion

As illustrated in Fig 2, the RF frequency response of the adaptive splitter was measured by using a broadband vector network analyzer that supplied and swiped the frequency of the input RF signal driving the EOM.

Figure 3 shows the measured normalized RF spectrum coupled into the input fiber Port 9 coupled into the fiber input Port 9 as an input signal. Figure 3 demonstrates that the frequency response of the splitter is mainly limited by that of the EOM (bandwidth of 4 GHz) used in the experiments. The ratios of output power level at fiber Port 10 was to the output power levels Ports 1-4 were maintained constant, while the optical power at Port 10 was amplified via an EDFA, then coupled into Port 11 for subsequent splitting into the output fiber Ports 5-8.

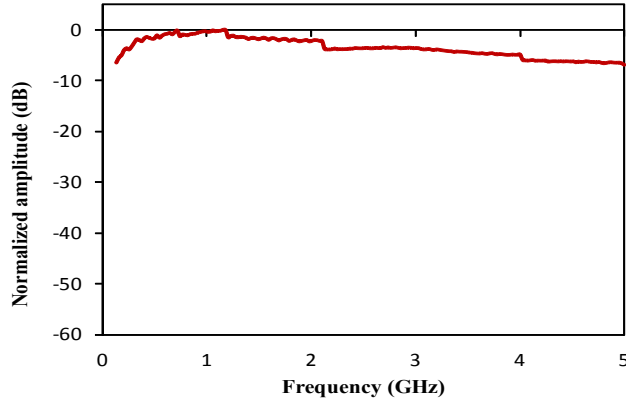


Fig 3. Measured normalized RF spectrum coupled into the input fiber Port 9.

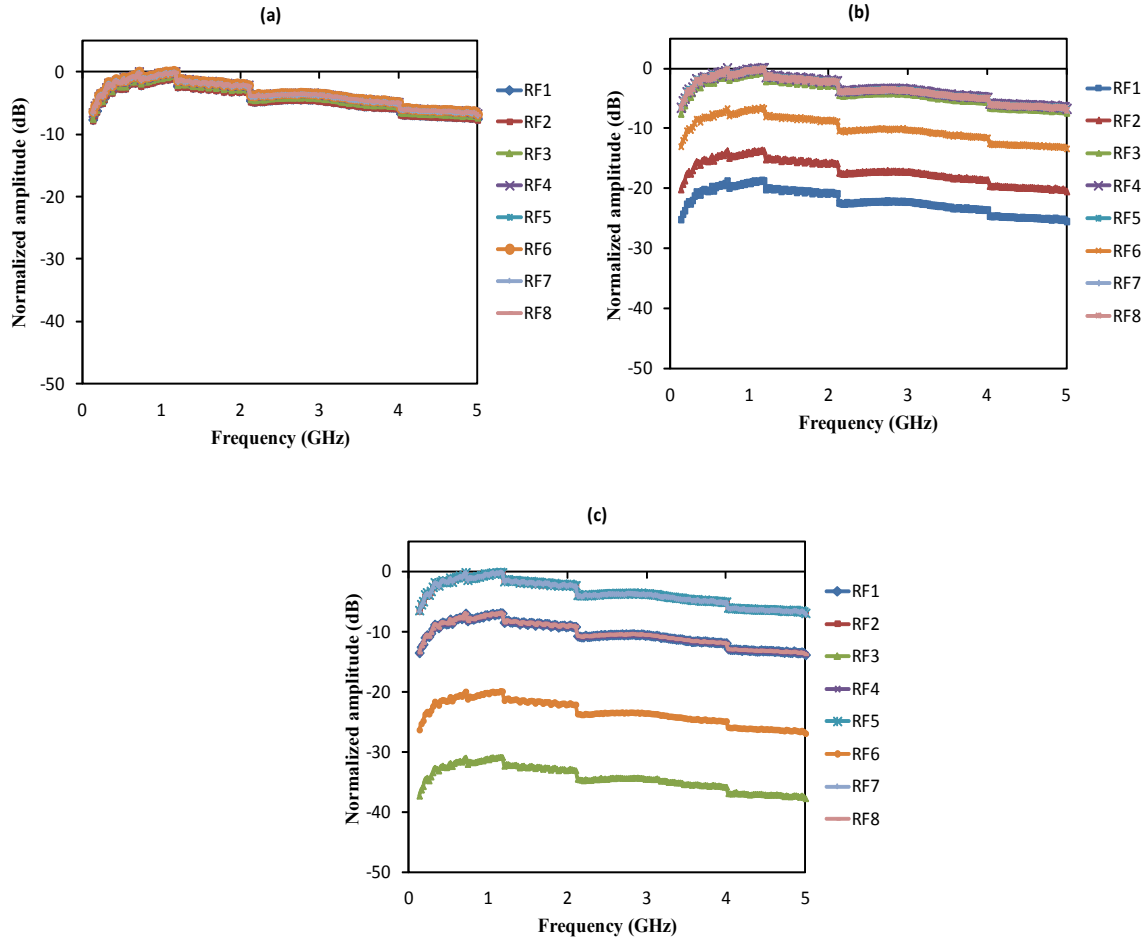


Fig 4. Measured normalized RF spectrum coupled with the output RF Ports1-8, for an input RF frequency range from 130 kHz to 5GHz. Splitting was achieved by uploading multicasting holograms onto the Opto-VLSI processor, corresponding to different normalized RF power splitting ratios: (a) 1.00:1.00:1.00:1.00:1.00:1.00:1.00:1.00, (b) 0.01:0.04:1.0:1.00:1.00:0.23:1.00:1.00, and (c) 0.20:1.00:0.00:0.20:1.00:0.01:1.00:0.20.

Figure 4 shows the frequency responses of the splitter for different splitting scenarios, over a frequency range from 130 kHz to 5 GHz. For each desired splitting profile, optimized multicasting phase holograms were generated (using simulated annealing algorithms) and applied onto the corresponding pixels blocks. Figure 4(a) demonstrates a scenario where the input RF power is split equally into the output Ports 1-8 by uploading two different computer-generated phase holograms corresponding to an RF splitting profile 1.00:1.00:1.00:1.00:1.00:1.00:1.00:1.00, resulting in a uniform RF responses for all the output Ports 1-8. Figure 4(b) shows the measured output Port 1-8 RF responses when the power levels at Ports 1, 2, and 6 were reduced by 18dB, 13dB, and 7dB, respectively, by uploading computer-generated phase holograms onto the Opto-VLSI processor, which correspond to an RF splitting profile of 0.01:0.04:1.0:1.00:1.00:0.23:1.00:1.00.

Figure 4(c) shows the measured RF responses when the power levels at Port 3 and Port 6 were suppressed by 30dB and 20dB, respectively, while those at Ports 1, 4, and 8 were reduced by 7dB, corresponding to a splitting profile of 0.20:1.00:0.00:0.20:1.00:0.01:1.00:0.20. The experimental results shown in Figure 4 demonstrate the ability of the proposed broadband adaptive RF splitter structure, shown in Figure 2, to realize arbitrary RF splitting ratios through the use of optimized multicasting phase holograms uploaded onto the Opto-VLSI processor. Note that the measured maximum output power fluctuation for the output ports was less than 2.0 dB. Also, the measured crosstalk level was less than -30 dB. Note also that, by using the erbium-doped fiber amplifier (EDFA), the insertion losses of the proposed RF splitter was compensated. Finally, it is noticed that the measured output RF power splitting ratios are in excellent agreement with the user-defined ratios used in the computer algorithm that was especially developed to generate the optimized multicasting phase holograms.

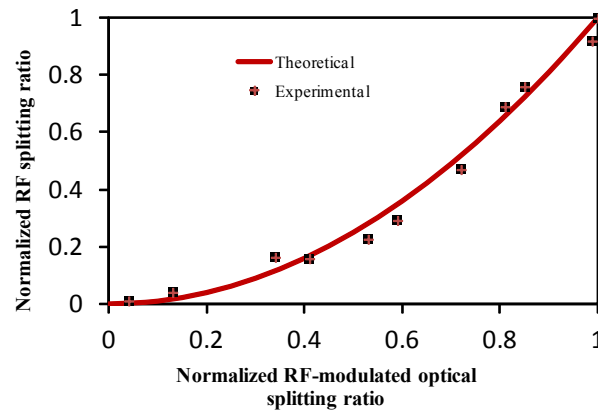


Fig 5. Measured and theoretical RF splitting ratio versus optical splitting ratio for Port 3.

Figure 5 shows the measured normalized RF splitting ratio, versus the normalized optical splitting ratio. Port 3 was selected to demonstrate the quadratic relationship between the RF and optical splitting ratios expressed in Eq (2). It is clear that the experimental results are in excellent agreement with the simulation results generated by the theoretical relationship of the RF and optical power splitting ratios governed by Eq (2). Note that the constant A in Eq (2) can be set to a unity value by controlling the EDFA gain. The results displayed in Figs 3-5 demonstrate the principle of the proposed multi-port broadband adaptive RF power splitter.

5 Conclusion

A 1×8 broadband adaptive RF power splitter structure employing an Opto-VLSI processor in conjunction with a 4-f imaging system array has been proposed and experimentally demonstrated. Several RF signal splitting scenarios have been investigated, and experimental results have shown that an input RF signal can arbitrarily be split into eight output ports by simply uploading optimized multicasting phase

holograms onto the Opto-VLSI processor. A crosstalk level below -30 dB has experimentally been measured. Negligible insertion losses have been achieved by using an erbium-doped fiber amplifier (EDFA), making the proposed adaptive RF splitter attractive for many RF applications, including RF signal processing.

References

1. Minasian R A, Alameh K, Optical-Fiber Grating –Based Beamforming Network for Microwave Phased Arrays, *IEEE Trans Microwave Theory and Techniques*, 45(1997)1513-1518.
2. Minasian R A, Alameh K, High capacity optical beam forming for phased arrays with fiber gratings and frequency conversion for beat noise control, *Appl Opt*, 38(1999)4665-4670.
3. Yi X, Huang T X H, Minasian R A, Photonic beamforming based on programmable phase shifter with amplitude and phase control, *IEEE Photonic Technology Lett*, 23(2011)1286-1288.
4. Minasian R A, Alameh K E, Wavelength-multiplexed photonic beam-former architecture for microwave phased arrays, *Microwave and Optical Technology Lett*, 10(1995)84-87.
5. Alameh K E, Minasian R A, Fourikis N, High Capacity Optical Interconnects for Phased Arrays Beamformers, *IEEE J Lightw Technol*, 13(1995)1116-1120.
6. Jalalifar M, Uddin M J, Power splitter architecture and applications, *Progress in Electromagnetics Research C*, 18(2011)231-244.
7. Uddin M J, Ibrahimy M I, Reaz M B I, Development of Power Control Module in RFID Reader Circuit: A Mentor Graphic Simulation Approach, *Proceedings of the International Conference on Computer and Communication Engineering 2008*, Kuala Lumpur, Malaysia, 13-15(2008)1167-1171.
8. Racanelli M, Kempf P, SiGeBiCMOS Technology for Communication Products, *Proc IEEE CICC*, 2003, pp 331-334.
9. Lu L-H, Liao Y-T, Wu C-R, A Miniaturized wilkinson power divider with CMOS active inductors, *IEEE Microwave and Wireless Components Lett*, 15(2005)775-777.
10. Barea A H, Robertson I D, Monolithic MESFET distributed baluns based on the distributed amplifier gate-line termination technique, *IEEE Trans Microw Theory Tech*, 45(1997)188-195.
11. Chiu J-C, Lin J-M, Wang Y-H, A Novel Planar Three-Way Power Divider, *IEEE Microwave and Wireless Components Lett*, 16(2006)449-451
12. Lee S Y, Lai C C, A 1-V wideband low-power CMOS active differential power splitter for wireless communication, *IEEE Trans Microw Theory Tech*, 55(2007)1593-1600.
13. Mao S-G, Chueh Y-Z, Broadband Composite Right/Left-Handed Coplanar Waveguide Power Splitters With Arbitrary Phase Responses and Balun and Antenna Applications, *IEEE Trans antennas and propagation*, 54(2006)243-250.
14. Mustafa H A B, Xiao F, Alameh K, Opto-VLSI-based variable RF power splitter, *EEE Proceedings of the International Conference on High-Capacity Optical Networks & Emerging/Enabling technologies 2012*, Istanbul, Turkey, December 12-14, 2012.
15. Xiao F, Juswardy B, Alameh K, Tunable photonic microwave filters based on Opto-VLSI processors, *IEEE Photon Technol Lett*, 21(2009)751-753.
16. Mustafa H, Xiao F, Alameh K, Reconfigurable optical power splitter/combiner based on Opto-VLSI processing, *Opt Express*, 19(2011)21890-21897.
17. Ahderom S T, Raisi M, Alameh K, Eshraghian K, Testing and Analysis of Computer Generated Holograms for MicroPhotonics Devices, in *Proceeding of the second IEEE international Workshop on Electronic design, Test and applications (DELTA'04)*, Perth, Australia, Jan 28-30, 2004, pp 47-52.
18. Zheng R, Wang Z, Alameh K, Crossland W A, An opto-VLSI reconfigurable broad-band optical splitter, *IEEE Photonics Technology Lett*, 17(2005)339-341.
19. Xiao Feng, Alameh Kamal, Lee Yong Tak, Tunable multi-wavelength fiber lasers based on an Opto-VLSI processor and optical amplifiers, *Opt Exp*, 17(2009)23123-23129.
20. Xiao Feng, Alameh Kamal, Lee Yong Tak, Opto-VLSI-based tunable single-mode fiber laser, *Opt Exp*, 17(2009)18676-18680.
21. Ahderom S, Raisi M, Alameh K, Eshraghian K, Dynamic WDM equalizer using Opto-VLSI beam processing, *IEEE Photon, Technol Lett*, 15(2003)1603-1605, .

[Received : 20.11.2014 ; accepted : 11.12.2014]